Direct Observation of the Push Effect on the O–O Bond Cleavage of Acylperoxoiron(III) Porphyrin Complexes

Kazuya Yamaguchi, Yoshihito Watanabe,* and Isao Morishima*

Contribution from the Division of Molecular Engineering, Graduate School of Engineering, Kyoto University, Kyoto 606-01, Japan

Received November 16, 1992

Abstract: The first direct observation of the push effect on heterolytic and homolytic O–O bond cleavage steps of acylperoxoiron(III) porphyrin complexes is reported for a series of acylperoxoiron(III) porphyrins (**5**) having substituents at the meso-positions of the porphyrin ring. Transformation of **5** to the corresponding oxoferryl (O=Fe^{IV}) porphyrin cation radicals (**6**) *in methylene chloride* at –80 °C by heterolytic O–O bond cleavage was found to be first order in [**5**]. Introduction of electron-donating substituents at the meso-positions of the porphyrin ring facilitates the O–O bond cleavage in **5**. Addition of 1 equiv of imidazole derivatives to a methylene chloride solution of **5** immediately gave an acylperoxoiron(III) porphyrin–imidazole adduct (**9**). The conversion of **9** to **6** was also found to be first order in [**9**], and the coordination of electron-rich imidazole derivatives strongly encouraged the O–O bond cleavage of **9**. On the other hand, the push effect on the homolytic O–O bond cleavage reaction has been examined *in toluene* at –6 °C to about –40 °C. The homolytic O–O bond cleavage of **9** afforded the imidazole adduct of oxoferryl porphyrin complex **7** when phenylperacetic acid was employed. Homolysis of the O–O bond is enhanced by the imidazole ligation; however, the push effect on homolysis is much less than that on heterolysis. These results explain the biological utilization of strong electron-donor ligands in heme enzymes such as peroxidase, cytochrome P-450, and catalase.

Introduction

In the oxygen activation by cytochrome P-450, peroxidase, and catalase, heterolytic O–O bond cleavage of hydroperoxoiron(III) porphyrin complexes is believed to afford oxoferryl porphyrin cation radical intermediates.[1] In fact, a reactive species called "Compound I" is observable in some peroxidase reactions.[2] For these heme enzymes, anionic proximal ligands are considered to be crucial to cause the heterolytic process by serving as a strong internal electron donor to destabilize the O–O bond of the hydroperoxoiron(III) porphyrin (push effect).[3-7] In 1976, Dawson et al. proposed that the thiolate ligand bound to the heme iron of P-450 pushes electron density into the hydroperoxide through iron(III), thereby weakening the O–O bond and facilitating its cleavage to give an oxoferryl porphyrin cation radical (Compound I).[8a] The proximal imidazolate ligand in peroxidase[4] and the phenolate ligand in catalase[5] are also expected to play a key role in the O–O bond cleavage reaction in a similar manner.[3,6,7] In addition, the distal environment surrounding the heme must play dominant role. In the case of cytochrome *c* peroxidase, the distal histidine could serve as a proton donor and work together with charged arginine to make the distal side substantially polar (pull effect). Consequently, these effects favor charge separation between two oxygens of the iron-bound peroxide (Figure 1).[8] P-450 would make up for the lack of the distal charged residue by having the proximal thiolate with full negative charge and therefore strong "push".

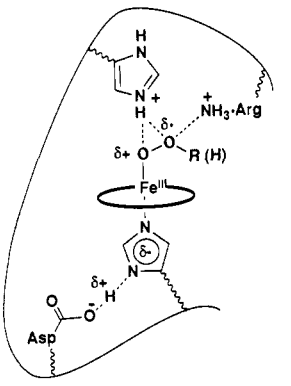

Figure 1. Schematic drawing of push–pull effect for the formation of Compound I of CCP.

The push–pull mechanism has been examined by several model systems.[9-11] Traylor et al. have examined the general acid/general base effects of imidazole in catalytic oxidation of 2,4,6-tri-*tert*-butylphenol by an iron porphyrin–peracid system.[9] Bruice et al. also reported the effects of imidazole and pH on the O–O bond cleavage reactions catalyzed by metalloporphyrins for similar

(1) For example: (a) White, R. E.; Coon, M. *J. Annu. Rev. Biochem.* **1980**, *50*, 315–356. (b) Ortiz de Montellano, P. R. In *Cytochrome* P-450; Ortiz de Montellano, P. R., Ed.; Plenum Press: New York, 1986; pp 217–271. (c) Dawson, J. H. *Science* **1988**, *240*, 433–439. (d) Watanabe, Y.; Groves, J. T. In *The Enzymes*; Sigman, Boyer, Eds.; Academic Press: Orlando, 1992; Vol. 20, pp 405–452.

(2) Dolphin, D.; Forman, A.; Borg, D. C.; Fajer, J.; Felton, R. H. *Proc. Natl. Acad. Sci. U.S.A.* **1971**, *68*, 614–618.

(3) Poulos, T. L.; Finzel, B. C.; Gunsalus, I. C.; Wagner, G. C.; Kraut, J. *J. Biol. Chem.* **1985**, *260*, 16122–16130.

(4) Thanabal, V.; de Ropp, J. S.; La Mar, G. N. *J. Am. Chem. Soc.* **1988**, *110*, 3027–3035.

(5) Murthy, M. R. N.; Reid, T. J., III; Sicignano, A.; Tanaka, N.; Rossmann, M. G. *J. Mol. Biol.* **1981**, *152*, 465–499.

(6) Poulos, T. L.; Finzel, B. C.; Howard, A. J. *Biochemistry* **1986**, *25*, 5314–5322.

(7) Poulos, T. L.; Howard, A. J. *Biochemistry* **1987**, *26*, 8165–8174.

(8) (a) Dawson, J. H.; Holm, R. H.; Trudell, J. R.; Barth, G.; Linder, R. E.; Bunnenberg, E.; Djerassi, C.; Tang, S. C. *J. Am. Chem. Soc.* **1976**, *98*, 3707–3709. (b) Poulos, T. L. *Adv. Inorg. Biochem.* **1987**, *7*, 1–36.

(9) (a) Traylor, T. G.; Lee, W. A.; Stynes, Dennis, V. *J. Am. Chem. Soc.* **1984**, *106*, 755–764. (b) Traylor, T. G.; Popovitz-Biro, R. *J. Am. Chem. Soc.* **1988**, *110*, 239–243. (c) Traylor, T. G.; Xu, F. *J. Am. Chem. Soc.* **1990**, *112*, 178–186.

(10) (a) Lee, W. A.; Bruice, T. C. *J. Am. Chem. Soc.* **1985**, *107*, 513–514. (b) Zipplies, M. Z.; Lee, W. A.; Bruice, T. C. *J. Am. Chem. Soc.* **1986**, *108*, 4433–4445. (c) Yuan, L.-C.; Bruice, T. C. *J. Am. Chem. Soc.* **1986**, *108*, 1643–1650. (d) Bruice, T. C.; Balasubramanian, P. N.; Lee, R. W.; Lindsay Smith, J. R. *J. Am. Chem. Soc.* **1988**, *110*, 7890–7892. (e) Panicucci, R.; Bruice, T. C. *J. Am. Chem. Soc.* **1990**, *112*, 6063–6071. (f) Gopinath, E.; Bruice, T. C. *J. Am. Chem. Soc.* **1991**, *113*, 4653–4665.

(11) (a) Groves, J. T.; Watanabe, Y. *Inorg. Chem.* **1986**, *25*, 4808–4810. (b) Groves, J. T.; Watanabe, Y. *J. Am. Chem. Soc.* **1986**, *108*, 7834–7836 and 7836–7837. (c) Groves, J. T.; Watanabe, Y. *J. Am. Chem. Soc.* **1988**, *110*, 8443–8452. (d) Labeque, R.; Marnett, L. J. *J. Am. Chem. Soc.* **1989**, *111*, 6621–6627. (e) Higuchi, T.; Uzu, S.; Hirobe, M. *J. Am. Chem. Soc.* **1990**, *112*, 7051–7053. (f) Robert, A.; Loock, B.; Momenteau, M.; Meunier, B. *Inorg. Chem.* **1991**, *30*, 706–711. (g) Yamaguchi, K.; Watanabe, Y.; Morishima, I. *Inorg. Chem.* **1992**, *31*, 156–157.

0002-7863/93/1515-4058$04.00/0

Scheme I

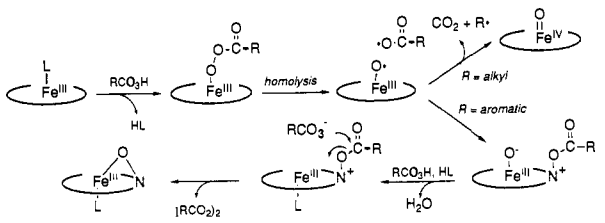

catalytic systems in aqueous solutions.[10] In the latter case, enhancement of the oxidation rate at high pH could be attributed to facile homolytic O–O bond cleavage of alkylperoxoiron(III) porphyrin due to the alteration of the sixth axial ligand from H_2O to HO^-.[10e,f] While these kinetic studies seem very important to understanding the O–O bond scission reactions, the rate constants (k_{obs}) in these studies include preequilibrium constants as shown in eq 1, where X represents either H_2O or ^-OH depending on the

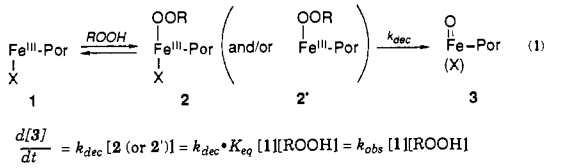

pH of the solution.[10b,d-f] On the other hand, we have reported the rate constants (k_{dec}) of the O–O bond cleavage step by direct observation of the conversion of acylperoxoiron(III) porphyrins to the corresponding high-valent complexes at low temperature.[11a-c,g] In the course of these studies, we have demonstrated that homolytic and heterolytic O–O bond cleavage mechanisms are controlled by changing the solvent from CH_2Cl_2 (*heterolysis*) to toluene (*homolysis*).[11b,c,12] For instance, the reaction of Fe^{III}-TMP(OH) (**4**)[13] with *m*-chloroperoxybenzoic acid (*m*CPBA) *in* CH_2Cl_2 at low temperature gives an Fe^{III}–*m*CPBA adduct (**5**-*m*CPBA) as an irreversible process followed by the formation of the corresponding oxoferryl cation radical complex (**6**) due to the heterolytic O–O bond cleavage (eq 2).[11b,c] Therefore, the first-

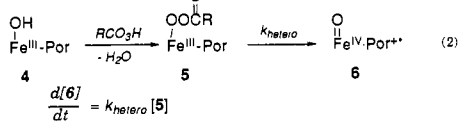

order rate constants (k_{hetero}) for the formation of **6** are directly observed in these reactions. On the contrary, the same reaction in toluene gives the homolytic O–O bond cleavage product of **5**-*m*CPBA. In the latter case, final products are dependent on the structure of peracids employed, i.e., alkyl peracids directly form the O=Fe^{IV} porphyrin **7** according to rapid decarboxylation[14] of the radical intermediate RCOO•. On the other hand, aromatic peracids such as perbenzoic acid give Fe(III) porphyrin *N*-oxides (**8**) with concomitant formation of dibenzoyl peroxides by consuming 2 mol of peracid. These homolytic O–O bond cleavage reaction mechanisms are illustrated in Scheme I.[11b,c] Apparently, the polarity of the solvent is very important to the nature of the O–O bond cleavage, consistent with the proposed role of distal arginine in cytochrome *c* peroxidase (CCP) reaction.[8]

Direct observation of **5** in these homolytic and heterolytic O–O bond cleavage reactions enables us to examine further details of these reactions, especially *the push effect*. In order to understand the push effect on the heterolysis and homolysis of the O–O bond,

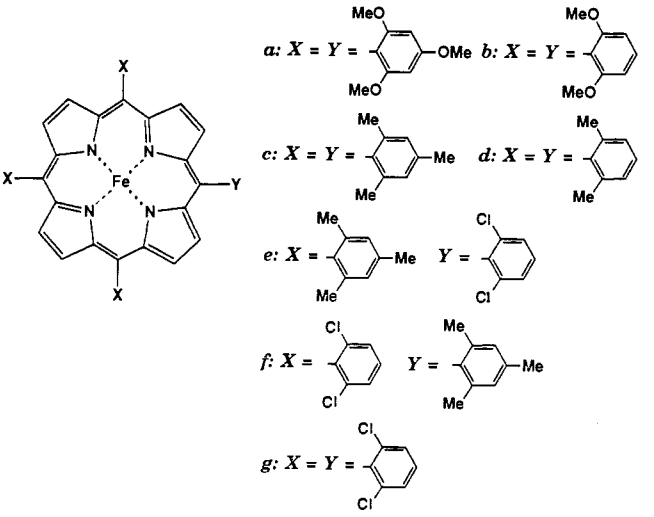

Figure 2. Structures of substituted iron porphyrin complexes (**a–g**) employed in this study. Axial ligands are omitted for simplicity.

we have prepared a series of **5** having substituents at the meso-positions of the porphyrin ring as shown in Figure 2. Further, the enhancement of reactivity of **5** by the introduction of a series of imidazoles as the sixth ligand has been examined. These studies allow quantitative analyses of the push effect of both the substituents at the meso-positions of the porphyrin ring and the sixth ligand on the O–O bond cleavage reactions.

Experimental Section

Materials. Methylene chloride and toluene were distilled from CaH_2 and stored under argon. Chloroform was distilled from potassium bicarbonate before use. 1-Methylimidazole, 1-phenylimidazole, and 1-methyl-5-chloroimidazole were purchased from Aldrich Chemical Co. and used without further purification. 3-Chloroperoxybenzoic acid (*m*CPBA) was purchased from Nacalai Tesque. 4-Nitroperoxybenzoic acid (*p*NPBA) was prepared according to literature procedures.[15] Peroxybenzoic acids were purified by washing with phosphate buffer (pH 7.4).[16] Phenylperoxyacetic acid (PPAA) was prepared and purified according to literature procedures.[11c] Highly concentrated hydrogen peroxide was prepared by vacuum evaporation of water from aqueous H_2O_2 (30%) at 0 °C. Other commercially available chemicals were purchased and used without further purification.

Preparation of Porphyrins. Tetramesitylporphyrin [$TMPH_2$], tetrakis-(2,6-dimethylphenyl)porphyrin [$TDMPPH_2$], and other porphyrins having substituents at the meso-positions were prepared by modification of methods reported.[17] Porphyrins unsymmetrically substituted with 2,6-dichlorophenyl and mesityl groups were prepared as follows.

A chloroform solution (1 L) containing mesitaldehyde (0.8 mL, 5.4 mmol), 2,6-dichlorobenzaldehyde (0.875 g, 5.0 mmol), pyrrole (0.7 mL, 10.9 mmol), $Et_2O{\cdot}BF_3$ (1.0 mL, 8.1 mmol), and 10 mL of ethanol was refluxed for 1 h under N_2 atmosphere. To the resulting solution was added 1.8 g of tetrachloro-1,4-benzoquinone (7.3 mmol), and the solution was refluxed for 1 h. 5,10,15-Trismesityl-20-(2,6-dichlorophenyl)-porphyrin (**e**) and 5,10,15-tris(2,6-dichlorophenyl)-20-mesitylporphyrin (**f**) were isolated by SiO_2 column chromatography (CH_2Cl_2:hexane = 4:6). For **e**, ^1H NMR ($CDCl_3$) δ: pyrrole 8.69 (d, J = 4.5, 2 H), 8.63 (s, 4 H), 8.60 (d, J = 4.8, 2 H); *m*-H 7.79 (d, J = 7.8, 2 H), 7.28 (br s, 6 H); *p*-H 7.70 (t, J = 6.6, 1 H); *p*-Me 2.63 (s, 9 H); *o*-Me 1.87 (s, 18 H); N–H –2.47 (s, 2 H). FABMS: *m/e* 808 (M^+, 100), 810 (M^+ + 2, 107), 812 (M^+ + 4, 38). For **f**, ^1H NMR ($CDCl_3$) δ: pyrrole 8.70 (d, J = 4.8, 2 H), 8.67 (s, 4 H), 8.61 (d, J = 4.8, 2 H); *m*-H 7.80 (d, J = 7.9, 6 H), 7.28 (br s, 2 H); *p*-H 7.70 (t, J = 7.0, 3 H); *p*-Me 2.64 (s, 3 H); *o*-H 1.87 (s, 6 H); N–H –2.48 (s, 2 H). FABMS: *m/e* 860 (M^+, 100), 862 (M^+ + 2, 191), 864 (M^+ + 4, 196), 866 (M^+ + 6, 107), 868 (M^+ + 8, 49).

Iron was inserted in the porphyrins to form ferric porphyrin chloride complexes by a standard method.[18] Iron(III) porphyrins bearing hydroxo

(12) Watanabe, Y.; Yamaguchi, K.; Morishima, I.; Takehira, K.; Shimizu, M.; Hayakawa, T.; Orita, H. *Inorg. Chem.* **1991**, *30*, 2581–2582.
(13) Fe(III)TMP: 5,10,15,20-tetramesitylporphyrinatoiron(III).
(14) (a) Bevington, J. C.; Toole, J. *J. Polym. Sci.* **1958**, *28*, 413–420. (b) Braun, W.; Rajbenbach, L.; Eiricj, F. R. *J. Phys. Chem.* **1962**, *66*, 1591–1595. (c) Detar, D. F. *J. Am. Chem. Soc.* **1976**, *89*, 4058–4068.
(15) Silbert, L. S.; Siegel, E.; Swern, D. *J. Org. Chem.* **1962**, *27*, 1336.
(16) Schwartz, N. N.; Blumbergs, J. H. *J. Org. Chem.* **1964**, *29*, 1976.
(17) Lindsey, L. S.; Wagner, R. W. *J. Org. Chem.* **1989**, *54*, 828–836.

ligands were prepared by passing iron(III) porphyrin chloride through basic Al_2O_3 column chromatograph (eluent EtOAc) before use.[19]

Spectroscopy. Visible spectra were recorded on a Hitachi 330 spectrophotometer. Low-temperature absorption spectra were obtained by using a DN 1704 variable-temperature liquid nitrogen cryostat (Oxford Instruments). ESR spectra were obtained at 77 K with a JEOL JES-3X spectrometer operating with 100-kHz magnetic field modulation. FAB mass spectra were recorded on a JEOL SX-102A instrument.

Reaction of Fe^{III}(OH) Porphyrins with Peracids. In a typical reaction, a methylene chloride solution of Fe^{III}(OH) porphyrin (**4**, 2.0×10^{-5} M, 4 mL) in a 1-cm UV cuvette was placed in a cryostat unit of the UV–vis spectrophotometer. After equilibrium of the solution to the desired temperature, methylene chloride containing 1.2 equiv of peracid (9.6×10^{-5} mmol) was introduced in one portion. The reaction was monitored either by recording repetitive scans (scan rate 120 nm/min) or by recording absorption vs time at a fixed wavelength. Reactions of **4** with peracids in toluene were carried out and monitored in the same way.

Reaction of Peracid–Fe(III) Adducts with Imidazole Derivatives. Immediately after the mixing of **4** and peracid at −80 °C as described above, the formation of a peracid–Fe(III) porphyrin complex (**5**) was confirmed by UV–vis spectroscopy. A methylene chloride solution of 1 equiv amount of imidazole was then injected in one portion of the resulting solution. The reaction was monitored either by recording repetitive scans or by recording absorption vs time at a fixed wavelength. Reactions of toluene took place in the same way.

Preparation of EPR Samples. To a methylene chloride solution of TDMPPFe^{III}(OH) (**4d**, 8.0×10^{-3} M, 300 μL) was added 1 equiv of *m*CPBA (2.4×10^{-1} M, 10 μL) at −78 °C. The reaction mixture was frozen for EPR measurement. In a separate experiment, 1-phenylimidazole 2.4×10^{-1} M, 10 μL) was added immediately after the introduction of *m*CPBA, and the resulting solution was frozen for the measurement. The same reaction was carried out in toluene under the condition described above.

Results

I. Reactivity of Acylperoxoiron(III) Porphyrins Bearing a Series of Substituents at the Meso-Position of the Porphyrin Ring. A. Kinetics for the Formation of Oxoferryl Porphyrin Cation Radical in CH_2Cl_2. Reactions of hydroxoiron(III) porphyrins (**4**) listed in Figure 2 and *p*-nitroperbenzoic acid (*p*NPBA) took place in methylene chloride at −80 °C. The time course of the reaction was directly observed by UV–vis spectroscopy. For instance, the solution of hydroxoiron(III)TDMPP[20] (**4d**) was cooled to −80 °C in a UV–vis cuvette. Introduction of 3 equiv of *p*NPBA to the solution instantaneously afforded the corresponding acylperoxoiron(III) porphyrin (**5d**-*p*NPBA), which exhibits a typical visible spectrum of five-coordinated high-spin iron(III) porphyrins as shown in Figure 3. The following isosbestic changes of **5d**-*p*NPBA gave an oxoferryl porphyrin cation radical (**6d**), which exhibits a visible spectrum almost identical to that reported for O=Fe^{IV}TMP$^{+\cdot}$[11b,c] (Figure 3).

Trace A in Figure 3 shows the time course of absorbance change of **4d** at 415 nm upon the addition of 3 equiv of *p*NPBA. Similar spectral changes were also observed in the reactions of **4a–f** with peracids under the same conditions. On the basis of the spectral changes, the O–O bond cleavage of **5**-*p*NPBA was found to be first-order in [**5**-*p*NPBA] ($d[\mathbf{6}]/dt = k_{hetero}$ [**5**-*p*NPBA]) as shown in Figure 3 (inset), consistent with recent observations by Groves and Watanabe.[11c] The rate constants (k_{hetero}) for the substituted porphyrins are summarized in Table I. Electron-donating groups at the meso-positions of the porphyrin ring evidently accelerate the O–O bond cleavage step, whereas electron-withdrawing substituents retard the formation of **6**. In addition, **5**-*p*NPBA decomposes faster than the corresponding **5**-*m*CPBA, as expected for the heterolytic O–O cleavage in **5** (pull effect).[11c]

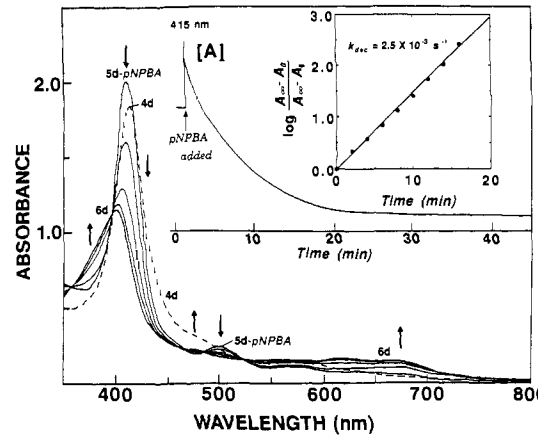

Figure 3. Visible spectral changes in the reaction of hydroxoiron(III) porphyrin (**4d**, – – –) and 3 equiv of *p*-nitroperoxybenzoic acid in methylene chloride at −80 °C. The spectrum of **5d**-*p*NPBA was recorded immediately after the addition of *p*-nitroperoxybenzoic acid. Line A represents the time-dependent changes of absorbance at 415 nm. Inset: plots of $\log(A - A_0)/(A - A_t)$ at 415 nm vs time for the formation of **6d** from **5d**-*p*NPBA.

Table I. Substituent Effect on First-Order Rate Constants for Heterolytic O–O Bond Cleavage Reactions of **5** in CH_2Cl_2 at −80 °C

	$10^3 k_{dec}$ (s^{-1}) ($\log k_{rel}$[c])	
complex[b]	*m*CPBA[d]	*p*NPBA[e]
5a	16.6 (0.71)	50.8 (0.66)
5b	4.0 (0.10)	14.5 (0.11)
5c	3.2 (0.00)	11.2 (0.00)
5d	0.3 (−1.03)	2.5 (−0.65)
5e	0.5 (−0.81)	2.2 (−0.71)
5f	*a*	0.6 (−1.27)

[a] Not available. [b] See Figure 1. [c] k_{rel} is the relative rate constant based on that of **5c**. [d] 3 equiv of *m*CPBA acid were used. [e] 3 equiv of *p*NPBA were used.

B. Kinetics for the Formation of Oxoferryl Porphyrin and Ferric Porphyrin *N*-Oxide in Toluene. As described in Scheme I, homolysis of the O–O bond in **5** gives either **7** or **8**, depending on the structure of peracid used. Thus the effect of substituents at the meso-positions on the O–O bond cleavage was examined by the use of phenylperoxyacetic acid (PPAA) and *m*CPBA. In both cases, the rate-determining steps are known to be the O–O bond cleavage step; however, the rate constants for the formation of **7** and **8** are distinguished as k_{homo1} and k_{homo2}, respectively (eq 3).

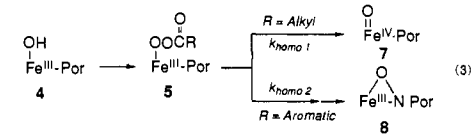

The reaction of **4d** and 1.2 equiv of PPAA was monitored by UV–vis spectroscopy at −40 °C *in toluene*. Introduction of PPAA to the solution afforded Fe^{III}TDMPP(PPAA) (**5d**-PPAA) at once, and the following transformation of **5d**-PPAA to the corresponding oxoferryl porphyrin **7d** with several isosbestic points was shown in Figure 4. Rapid formation of an intermediate followed by slow reaction is further demonstrated by the measurement of the time course of absorbance change at 536 nm upon the addition of 1.0 equiv of PPAA (Figure 4, inset). On the basis of the spectral changes, the rate of the formation of **7d** was found to be first-order in [**5d**-PPAA] ($d[\mathbf{7d}]/dt = k_{homo1}$ [**5d**-PPAA]). Similar spectral changes were also observed in the reactions of other substituted iron porphyrins with PPAA under the conditions described above. The rate constants (k_{homo1}) for the formation of **7** are summarized in Table II.

(18) Kobayashi, H.; Higuchi, T.; Kaizu, Y.; Osada, H.; Aoki, M. *Bull. Chem. Soc. Jpn.* **1975**, *48*, 3137.
(19) Woon, T. C.; Shirazi, A.; Bruice, T. C. *Inorg. Chem.* **1986**, *25*, 3845–3846.
(20) TDMPP = 5,10,15,20-tetrakis(2,6-dimethylphenyl)porphyrin.

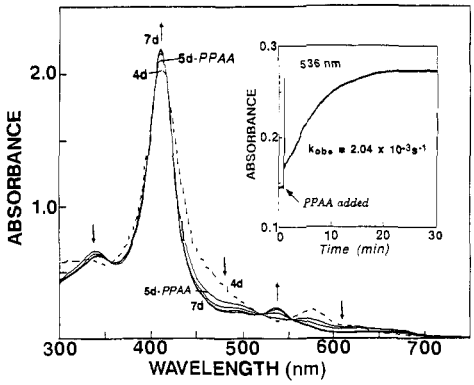

Figure 4. Visible spectral changes in the reaction of hydroxoiron(III) porphyrin (**4d**, - - -) and 1.2 equiv of phenylperoxyacetic acid in toluene at -40 °C. The spectrum of **5d**-PPAA was recorded immediately after the addition of PPAA. Inset: time-dependent changes of absorbance at 536 nm.

Table II. Substituent Effect on the Rate Constants for Homolytic O–O Bond Cleavage Reactions of **5** in Toluene

complex[a]	$10^3 k_{homo1}$ (s^{-1}) ($\log k_{rel}$)[b,d]	$10^{-9} k_{homo2}$ (mol^{-1} s^{-1}) ($\log k_{rel}$)[c,d]
5c	1.60 (0)	1.58 (0)
5d	2.04 (0.11)	1.56 (-0.06)
5e	2.14 (0.13)	1.67 (0.02)
5f	4.45 (0.44)	4.24 (0.43)
5g	6.31 (0.60)	4.89 (0.49)

[a] See Figure 1. [b] At -40 °C. [c] At -6 °C. [d] k_{rel} is the relative rate constant based on that of **5c**.

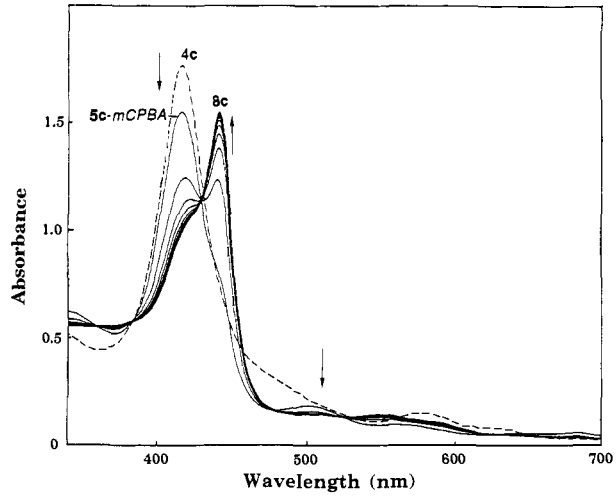

Figure 5. Time-dependent UV–vis spectral changes in the reaction of **4c** (- - -) and 3 equiv of *m*CPBA in toluene at -6 °C. The spectrum of **5c**-*m*CPBA was recorded immediately after the addition of *m*CPBA.

The reaction of **4c** with 3 equiv of *m*CPBA was also examined in toluene at -6 °C. As reported before, the reaction affords ferric porphyrin *N*-oxide (**8c**) via an intermediate (**5c**-*m*CPBA), as shown in Figure 5.[10c] The observation of **5c**-*m*CPBA as the sole intermediate supports the O–O bond cleavage step being the rate-determining. Figure 6A shows time-dependent absorbance change in the reaction of **4e** and *m*CPBA. Under the condition, the formation of **8** from **5**-*m*CPBA was found to be first-order both in [**5**-*m*CPBA] and in *peroxy acid remaining in the reaction solution* ($d[8]/dt = k_{homo2}$ [**5**-*m*CPBA][*m*CPBA]) as shown in Figure 6B. The rate constants (k_{homo2}) for substituted porphyrins are listed in Table II.

II. Effect of the Sixth Ligand on the O–O Bond Cleavage. A. Effect on Heterolysis of the O–O Bond. Introduction of 1.2 equiv of *m*CPBA to a methylene chloride solution of **4d** (2.0×10^{-5} M) at -80 °C in a UV–vis cuvette forms **5d**-*m*CPBA; followed by

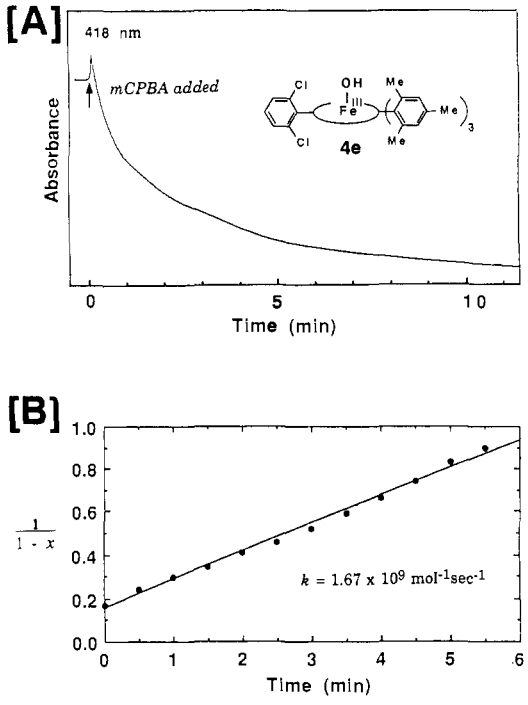

Figure 6. (A) Time-dependent changes of absorbance at 418 nm in the reaction of **4e** with 3 equiv of *m*CPBA in toluene at -6 °C. (B) Plots of $1/(1 - x)$, where x is the mole fraction of **8e** at 418 nm vs time for the formation of **8e**.

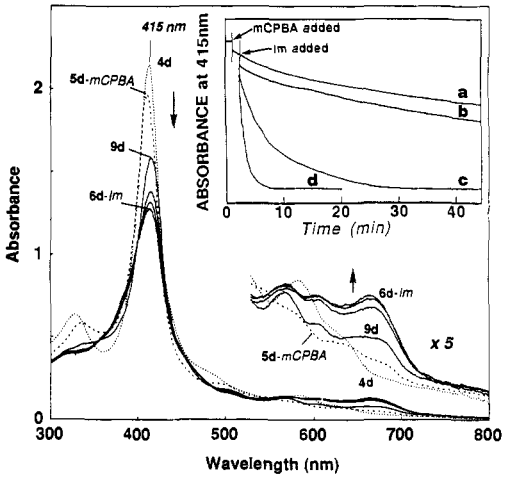

Figure 7. Visible spectral changes in the reaction of hydroxoiron(III) porphyrin (**4d**, ···) with 1.2 equiv of *m*CPBA acid and 1 equiv of 1-phenylimidazole in methylene chloride at -80 °C. The spectrum of **5d**-*m*CPBA (- - -) was recorded immediately after the addition of *m*CPBA and the spectrum of **9d** (—) was recorded immediately after the addition of 1-phenylimidazole. The conversion of **9d** to **6d**-Im was recorded every 5 min. Inset: time-dependent absorbance changes at 415 nm under the condition described above: a, without imidazole; b, with 1 equiv of 1-methyl-5-chloroimidazole; c, with 1 equiv of 1-phenylimidazole; d, with 1 equiv of 1-methylimidazole.

the heterolytic O–O bond cleavage, this reaction affords **6d** as observed above. Addition of 1 equiv of 1-phenylimidazole (1-PhIm) immediately after the formation of **5d**-*m*CPBA was found to give a new intermediate (**9d**), which exhibits a UV–vis spectrum typical of six-coordinated ferric low-spin complexes (Figure 7, λ_{max} for **9d** 416, 567, and 602 nm).[21-23] Further spectral change of **9d** to **6d**-Im (eq 4) was observed with several isosbestic points at 530, 487, 451, 398, and 354 nm.

(21) Ainscough, E. W.; Addison, A. W.; Dolphin, D.; James, B. R. *J. Am. Chem. Soc.* **1978**, *100*, 7585–7591.
(22) Quinn, R.; Nappa, M.; Valentine, J. S. *J. Am. Chem. Soc.* **1982**, *104*, 2588–2595.

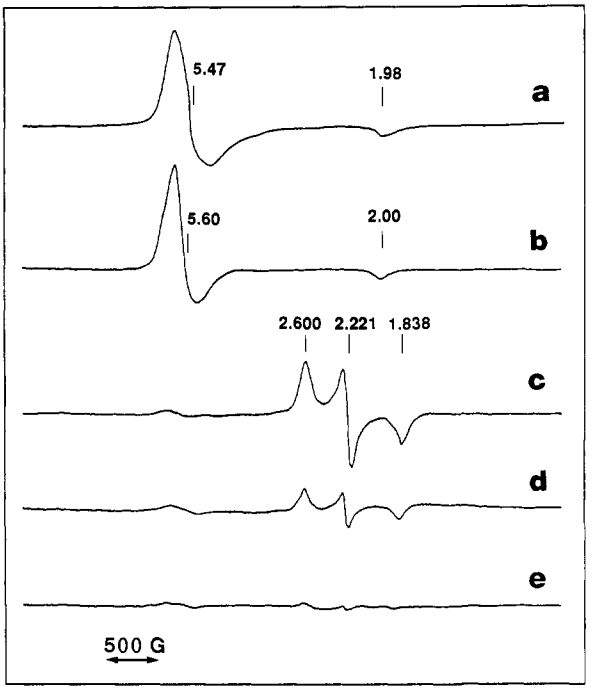

Figure 8. EPR spectral changes for the reaction of **4d** with 1.0 equiv of *m*CPBA: a, the spectrum of **4d**; b, immediately after the addition of *m*CPBA to the solution of a; c, **9d** formed by the addition of 1.0 equiv of 1-phenylimidazole to the sample of b; d and e, time-dependent EPR spectral changes of the solution of c (5-min interval).

Table III. Representative ESR Data for Various Iron Porphyrin Complexes

complex	solvent	ESR ⟨*g*⟩ values			ref
TDMPPFe^{III}(OH)	CH_2Cl_2	5.47		1.98	*a*
TDMPPFe^{III}(OH)	toluene	5.48		1.99	*a*
TDMPPFe^{III}(*m*CPBA)	CH_2Cl_2	5.60		2.00	*a*
TDMPPFe^{III}(PPAA)	toluene	5.75		2.00	*a*
TDMPPFe^{III}(*m*CPBA)(1-PhIm)	CH_2Cl_2	2.600	2.221	1.838	*a*
TDMPPFe^{III}(PPAA)(1-PhIm)	toluene	2.543	2.182	1.870	*a*
[TPPFe^{III}(ImH)$_2$]Cl	CH_2Cl_2	2.92	2.30	1.56	22
[TPPFe^{III}(4-MeImH)$_2$]Cl	CH_2Cl_2	2.87	2.29	1.54	22
TPPFe^{III}(ImH)(OO*n*-Bu)	CH_2Cl_2	2.352	2.194	1.935	23b
TPPFe^{III}(4-MeImH)(OO*n*-Bu)	CH_2Cl_2	2.344	2.195	1.935	23b
TPPFe^{III}(OMe)(OO*t*-Bu)	CH_2Cl_2	2.316	2.157	1.952	23a
PPIXDBFe^{III}(OAr)(1-MeIm)	toluene/ CH_2Cl_2	2.56	2.21	1.85	21
PPIXDBFe^{III}(OAr)(Py)	toluene/ CH_2Cl_2	2.61	2.19	1.84	21

[a] This work.

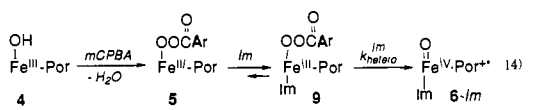

On the basis of stoichiometric formation, spectral features, and transformation of **9d** to **6d**-Im, **9d** is assigned to Fe^{III}TDMPP-(1-PhIm)(*m*CPBA). Further evidence for the stoichiometric formation of the acylperoxoiron(III)–imidazole adduct was obtained by EPR spectroscopy of **9d** at 77 K. Upon introduction of a stoichiometric amount of *m*CPBA to a CH_2Cl_2 solution of **4d** at −78 °C, a small EPR spectral change due to the replacement of fifth ligand was observed (Figure 8, **a** → **b**). Further addition of 1 equiv of 1-PhIm to the resulting solution gave an EPR spectrum characteristic of six-coordinated ferric low-spin complexes (**b** → **c**).[21-23] Finally, EPR signals disappeared according to the formation of **6d**[24] (**c** → **d** → **e**). The ⟨*g*⟩ values of **4d**, **5d**, **9d**, and some related low-spin complexes including PPIXDBEFe-(OAr)(1-MeIm),[21] TPPFe(ImH)$_2$Cl,[22] and TPPFe(Im)(OOBu)[23] are summarized in Table III. These stepwise reactions drawn in eq 4 are also confirmed by following the time course of absorbance changes at 415 nm (Figure 7, inset; trace **c**). Similar spectral changes were also observed in the reaction of **5d** with either 1-MeIm (trace **d**) or 1-Me-5-ClIm (trace **b**). On the basis of the spectral changes, the O–O bond cleavage reaction of **9d** was found to be first order in [**9d**]. The rate constants (k^{Im}_{hetero}) for the formation of **6d** in the presence of a series of imidazoles are summarized in Table IV.

Table IV. Substituent Effect of Imidazoles on First-Order Rate Constants for the O–O Bond Cleavage Reactions of **5d**

imidazole	$10^{-3}k^{Im}_{hetero}$ (s^{-1})[a]	$10^{-3}k^{Im}_{homo}$ (s^{-1})[b]
without Im	0.3	2.0
1-Me-5-ClIm	0.6	2.4
1-PhIm	2.0	3.3
1-MeIm	16.6	5.0

[a] 1.2 equiv of *m*CPBA acid was used in CH_2Cl_2 at −80 °C. [b] 1.2 equiv of PPAA was used in toluene at −40 °C.

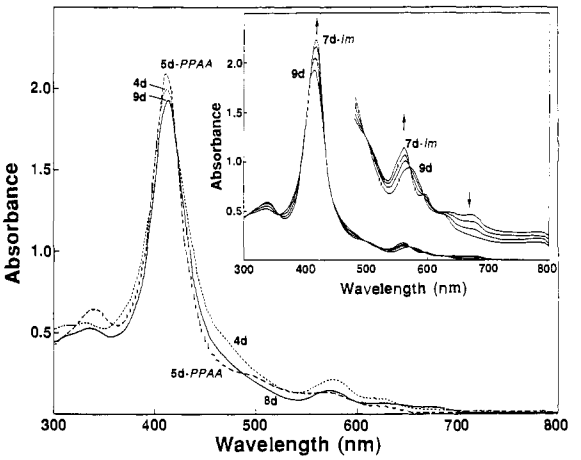

Figure 9. Visible spectral changes in the reaction of **4d** (···) with 1.2 equiv of PPAA and 1 equiv of 1-phenylimidazole in toluene at −40 °C. The spectrum of **5d**-PPAA (– – –) was recorded immediately after the addition of PPAA, and the subsequent addition of 1-phenylimidazole gave the spectrum of **9d** (—). Inset: time-dependent conversion of **9d** to **7d**.

B. Effect on Homolysis of the O–O Bond. The effect of the sixth ligand on homolysis of the O–O bond in **5d**-PPAA was also examined *in toluene*. For example, 1 equiv of 1-substituted imidazole was introduced immediately after the formation of **5d**-PPAA at −40 °C. As for the reactions in CH_2Cl_2, instantaneous formation of ferric low-spin intermediate **9d** was observed by UV–vis spectroscopy (λ_{max} 413 and 575 nm) as shown in Figure 9.

EPR measurement of **9d** in a separate experiment at 77 K showed ⟨*g*⟩ values at 2.543, 2.182, and 1.870, typical of ferric low-spin complexes. Finally, the conversion of **9d** to **7d**, whose UV–vis spectrum is almost identical to the authentic O=Fe^{IV}-TPP(ImH) complex reported by Balch et al.[25] (Figure 9, inset λ_{max} 418, 564, and 595 nm), was observed. These reaction cascades, summarized in eq 5, were visualized when the time course of the spectral changes was examined (Figure 10). By the

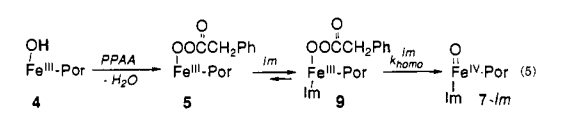

(23) (a) Tajima, K.; Jinno, J.; Ishizu, K.; Sakurai, H.; Ohya-Nishiguchi, H. *Inorg. Chem.* **1989**, *28*, 709–715. (b) Tajima, K. *Inorg. Chim. Acta* **1990**, *169*, 211–219.

(24) Groves, J. T.; Haushalter, R. C.; Nakamura, M.; Nemo, T. E.; Evans, B. J. *J. Am. Chem. Soc.* **1981**, *103*, 2884–2886.

(25) Chin, D. H.; Balch, A. L.; La Mar, G. N. *J. Am. Chem. Soc.* **1980**, *102*, 1446–1448 and 5945–5947.

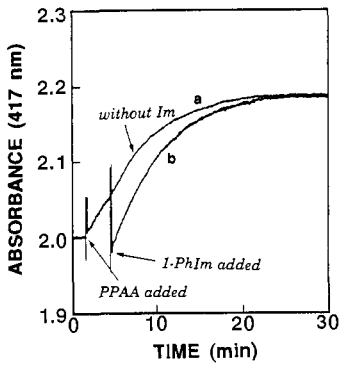

Figure 10. Time-dependent changes of absorbance at 417 nm under the condition described in Figure 9: a, without imidazole; b, with 1 equiv of 1-phenylimidazole.

inspection of Figure 10, the formation of **7d** was found to be first order in [**9d**], and the rate constants k^{Im}_{homo} for several substituted imidazoles are summarized in Table IV.

Discussion

Biological discrimination of peroxidase, catalase, and P-450 from hemoglobin, myoglobin, and cytochromes has been attributed to the ability of their anionic proximal ligands such as imidazolate, phenolate, and thiolate to facilitate heterolytic O–O bond cleavage in putative hydroperoxoiron(III) intermediates (push effect).[1c] Many efforts have been conducted to rationalize the push effect by using model systems, however, quantitative treatment of the push effect has been obstructed by difficulties in observing each reactive intermediate shown in eq 1.[9-11e,f] In the course of our model studies on the mechanism of oxygen activation by P-450 and peroxidase, we have observed many unstable intermediates postulated in the enzymatic reactions, including acylperoxoiron(III) complexes (**5**).[11a-c,g,1,26] More importantly, we have shown that homolysis and heterolysis of the O–O bond in **5** are differentiated by changing the solvent.[11b,c] Now we have focused our attention on the push effect on the O–O bond cleavage reactions. Thus, we have prepared iron porphyrins having a series of substituents at the meso-positions (Figure 2).[11g] These porphyrins are expected to serve to understand the push effect through the porphyrin ring. Further, reactions of **5** with imidazole derivatives have been carried out to examine the effect of sixth ligand. In the latter case, *N*-alkylimidazoles are employed, since imidazole and its derivatives bearing a free N–H moiety could serve as general acid catalysts,[9,10] while we like to see *only* the effect of imidazole as the sixth ligand.

Push Effect of the Sixth Ligand on Heterolysis of the O–O Bond. As reported before, the reaction of sterically hindered hydroxoiron(III) porphyrin with peracid in CH_2Cl_2 gave the corresponding oxoferryl porphyrin cation radical via the formation of an acylperoxoiron(III) porphyrin such as **5d** at low temperatures (Figure 3). Introduction of a stoichiometric amount of imidazole derivatives to **5d** afforded a new intermediate (**9d**) with the spin state changed from five-coordinated high spin to six-coordinated low spin. The spin-state change was confirmed by UV–vis and ESR spectral measurements (Figures 7 and 8). While **9d** is observable immediately after the addition of imidazole, a rapid isosbestic change of **9d** produces **6d**-Im even at –80 °C. We have assigned **6d**-Im as an oxoferryl cation radical with imidazole ligation, since the **6d** prepared without imidazole shows a Soret band at 410 nm while the Soret band of **6d**-Im appears at 414 nm (Figure 7). According to the formation of **9d** and its conversion to **6d**-Im in the stoichiometric reaction of **4d** with peracid and imidazole, **9d** is assigned as an acylperoxoiron(III)–imidazole ternary complex. **9d** exhibited ESR spectra with smaller $\langle g \rangle$ anisotropies ($\langle g \rangle$ = 2.600, 2.221, and 1.838 in CH_2Cl_2 and $\langle g \rangle$ = 2.543, 2.182. and 1.870 in toluene) than [TPPFe^{III}(ImH)$_2$]Cl ($\langle g \rangle$ = 2.92, 2.30, and 1.56 in CH_2Cl_2);[22] however, similar small anisotropies have been reported for TPPFe^{III}(OO*n*-Bu)(ImH), TPPFe^{III}(OMe)(OO*t*-Bu), and PPIXDBEFe^{III}(OAr)(1-MeIm) (Table III).[21,23]

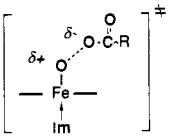

Figure 11. Push effect of the sixth ligand on the stabilization of the polar transition state in the heterolytic O–O cleavage reaction.

Table V. Temperature-Dependent Rate Constants for Heterolytic O–O Bond Cleavage Reactions of **5d**-*m*CPBA in the Presence and Absence of 1-PhIm

	$10^3 k^{(Im)}_{hetero}$ (s^{-1})	
t (°C)	without Im	1-PhIm
–40	3.94	11.2
–50	2.40	8.44
–60	1.28	5.52
–70	0.60	3.36
–80	0.30	2.00
–90	*a*	1.20

[a] Not available.

In order to study the kinetic profile of the reactions shown in eq 4, time courses of the reactions with a series of imidazole derivatives were monitored as absorbance changed at 415 nm. First-order rate constants (k^{Im}_{hetero}) summarized in Table IV indicate that electron-rich imidazoles accelerate the heterolytic O–O bond cleavage of **9**, whereas electron-poor imidazoles are less effective. Apparently, electron-rich imidazoles serve as a stronger electron donor (push) to stabilize the polar transition state as shown in Figure 11. It implies that anionic ligands such as imidazolate will be more effective for the O–O bond cleavage reaction. The activation energies for the O–O bond cleavage step of **5d**-*m*CPBA and **9d**-*m*CPBA were examined. On the basis of $k^{(Im)}_{hetero}$ values at various temperatures (Table V), the activation energies (E_a) in the presence and absence of 1-PhIm were calculated to be 3.9 and 5.9 kcal/mol, respectively. These results provide the first direct evidence for the proposed role of anionic proximal ligands in the O–O bond cleavage step of heme enzymes.

Push Effect of the Sixth Ligand on Homolysis of the O–O Bond. We have elucidated the push effect of the sixth ligand on the homolysis of the O–O bond in toluene. The reaction of Fe^{III}(OH) (**4**) and peracid is known to give either Fe(III) porphyrin *N*-oxide (**8**) or O=Fe^{IV} complex (**7**), depending on the structure of peracid used (Figures 4 and 5).[11b,c] The former reaction proceeds with consumption of 2 mol of aromatic peracids, whereas the latter requires 1 mol of alkyl peracids (Scheme I). Accordingly, the stability of acyloxyl radical and benzoyloxyl radical controls the final products, **7** and **8**. In order to avoid complicated side reactions such as protonation of imidazole by aromatic peracid remaining in the solution, we have chosen the latter system for further study. Incidentally, the reaction is too slow to examine at –80 °C, so homolysis of the O–O bond reactions were carried out at –40 °C.

When a stoichiometric amount of phenylperacetic acid (PPAA) was introduced to a toluene solution of **4d**, instantaneous formation of an acylperoxoiron(III) adduct (**5d**-PPAA) and a following relatively slow isosbestic change yielded oxoferryl porphyrin (**7d**) (Figure 4). Thus, the time course of the UV–vis spectral changes at 536 nm is evidently biphasic (Figure 4, inset). Further, the reaction of **5d**-PPAA with 1-phenylimidazole was examined by UV–vis spectroscopy (Figure 9), and immediate formation of an intermediate (**9d**) was observed. **9d** exhibits a characteristic UV–

(26) Yamaguchi, K.; Watanabe, Y.; Morishima, I. *J. Chem. Soc., Chem. Commun.* **1992**, *23*, 1709–1710.

Table VI. Temperature-Dependent Rate Constants for Homolytic O–O Bond Cleavage Reactions of **5d**-PPAA in the Presence and Absence of 1-PhIm

	$10^3 k_{homo}^{(Im)}$ (s^{-1})	
t (°C)	without Im	1-PhIm
–10	15.5	*a*
–20	7.1	11.8
–30	4.8	6.9
–40	2.0	3.3
–50	1.0	2.1
–60	*a*	1.0

[a] Not available.

vis spectrum of six-coordinated ferric low-spin complexes. Finally, **9d** decomposed to produce **7d** with several isosbestic points (Figure 9, inset). Time-dependent absorbance changes at 417 nm correspond to each step of the reactions (Figure 10). All these reactions proceeded with stoichiometric amounts of peracid and imidazole. Therefore, the six-coordinated ferric low-spin species is readily attributed to an acylperoxoiron(III)–Im complex. The EPR spectrum observed here for **9d** is very similar to that obtained in CH_2Cl_2 (Table III). The rate constants for k_{homo} and k_{homo}^{Im} (eqs 3 and 5) are summarized in Tables II and IV. Like the reactions in CH_2Cl_2, electron-rich imidazoles favor homolysis of the O–O bond by reducing the activation energy. For instance, the activation energies for homolysis of the O–O bond in **5d**-PPAA were calculated to be 6.6 and 7.9 kcal/mol in the presence and absence of 1-PhIm on the basis of $k_{homo}^{(Im)}$ values listed in Table VI. However, even in the case of 1-MeIm, the rate is not enhanced very much in toluene. For example, the ratio between k_{homo}^{Im} for 1-MeIm and that for 1-Me-5-ClIm is ca. 2.1 at –40 °C. It implies that the ratio of k_{homo}^{Im} at –80 °C is 3.7,[27] while the ratio of k_{hetero}^{Im} observed in CH_2Cl_2 at –80 °C is 28 (Table IV). Though we may not compare the absolute substituent effects of imidazole derivatives on homolysis and heterolysis since the solvent is different in these reactions, we believe that the smaller substituent effect on homolysis than that on heterolysis is reasonable due to the consideration as follows.

Roles of the Sixth Ligand in the O–O Bond Cleavage Reactions. Observed effects of substituted imidazoles on the O–O bond cleavage reactions are that (i) the coordination of imidazole to the acylperoxoiron(III) high-spin complex forming a low-spin species is not enough to enhance the O–O bond cleavage reactions and (ii) only electron-rich imidazoles are able to encourage the cleavage step.

Figure 12a shows idealized orbital interaction diagrams among iron, the axial ligand, and the peroxide of the six-coordinated porphyrin complex. The σ^* orbital of the iron-bound peroxide is overlapped with iron d_{yz} and d_{z^2} orbitals, which also interact with the p orbitals of the axial ligand. Thus, the push effect of the sixth ligand on the heterolytic and homolytic O–O bond cleavage can be explained by the orbital interaction between the sixth ligand and peroxide through iron. Electron donation (push) from the sixth ligand to the peroxide through iron results in electron distribution in the σ^* orbital of the peroxide, making the O–O bond labile. Apparently, this effect is favorable for both homolysis and heterolysis. On the other hand, the push effect by the sixth ligand causes the localization of the electron distribution in the σ^* orbital as shown in Figure 13. The localization of electron distribution in the σ^* orbital implies that the alcohol oxygen of the peroxide is negatively charged. The latter effect encourages the polar transition state (Figure 11) but rather discourages a nonpolar one (Fe–O•···•O–R). Accordingly, the push effect of imidazole assists the heterolytic O–O bond cleavage in two ways. On the other hand, the effect of imidazole on the homolytic O–O bond cleavage reaction is the result of two opposite factors. These considerations are consistent with the experimental results, i.e., while homolysis of the O–O bond is enhanced by the imidazole ligation, the push effect on homolysis is much less than that on heterolysis.

(27) The value is estimated according to the following equation:

$$k = Ae^{-\frac{E_a}{RT}}$$

where A values are assumed to be the same for both **9d**-1-MeIm and **9d**-1-Me-5-ClIm.

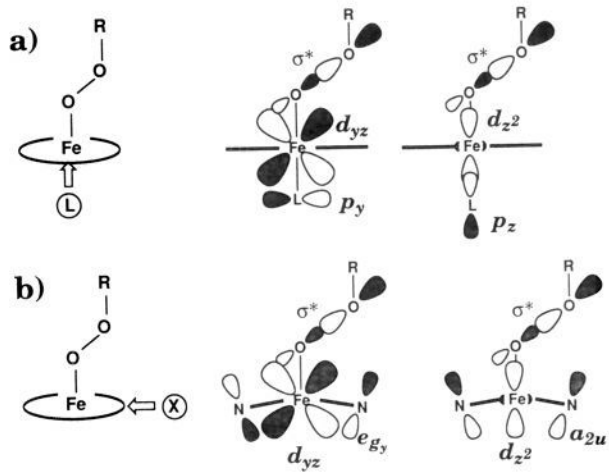

Figure 12. Idealized orbital interaction diagrams for five-coordinated and six-coordinated peroxoiron(III) porphyrin complexes: a, interaction of the sixth ligand's p orbitals, iron d orbitals, and the σ^* orbital of the peroxide; b, interaction among p orbitals of pyrrole nitrogens, iron d orbitals, and the σ^* orbital of the peroxide.

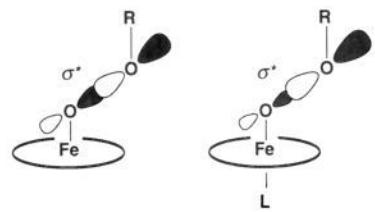

Figure 13. Polarized σ^*-orbitals of the peroxide bound to five- (left) and six-coordinated (right) iron.

Thus, the use of anionic proximal ligands such as thiolate and imidazolate in P-450 and peroxidase could predominantly enhance the heterolytic O–O bond cleavage process to afford Compound I. These conclusions are consistent with our recent site-directed mutagenesis study of human myoglobin, i.e., alteration of proximal histidine to cysteine causes the ligand change from imidazole to thiolate. According to the mutation, exclusive enhancement of the heterolytic O–O bond cleavage of cumene hydroperoxide over homolysis was observed.[28]

Push Effect by Substituents at the Meso-Positions of Porphyrin. Figure 12b shows the orbital interaction diagrams among iron, porphyrin, and the peroxide of the five-coordinated complex. The porphyrin e_g and a_{2u} orbitals of the five-coordinated domed porphyrin ring, where large electron densities are localized at the pyrrole nitrogens and the meso-carbons, interact with iron d_{xz}, d_{yz}, d_{z^2} and p_z orbitals, which also overlap with the σ^* orbital of the peroxide. Therefore, meso-substituents on a porphyrin ring are expected to affect the rate of the O–O bond cleavage of acylperoxoiron(III) porphyrin.

In the case of the heterolytic O–O bond cleavage reactions, electron-donating groups at the meso-positions of a porphyrin ring were found to accelerate the O–O bond cleavage step as shown in Table I, consistent with the push effect by the sixth

(28) (a) Adachi, S.; Nagano, S.; Watanabe, Y.; Ishimori, K.; Morishima, I. *Biochem. Biophys. Res. Commun.* **1991**, *180*, 138–144. (b) Adachi, S.; Nagano, S.; Ishimori, K.; Watanabe, Y.; Morishima, I.; Egawa, T.; Kitagawa, T.; Ryu Makino, R. *Biochemistry* **1993**, *32*, 241–252.

ligand. Accordingly, log k_{rel} correlates with the summation of Hammett σ values of the substituents ($\rho = -0.53$). As shown in Table II, however, the substituent effect on homolysis was found to be completely *opposite* that on heterolysis. In the homolytic O–O bond cleavage reactions, electron-donating groups at the meso-positions of a porphyrin ring were found to decelerate the O–O bond cleavage step. Both the reaction of **4** with *m*CPBA and that with PPAA give the same ρ value ($\rho = 0.15$). Accordingly, the reactions are considered to proceed with very similar transition states in toluene even though the final products are very different, consistent with the reaction mechanism shown in Scheme I. Discouragement of the homolysis by pushing the electron through the porphyrin ring is very different from the push effect observed by the sixth ligand. However, as discussed above, the push effect on the homolysis is divided into two opposite factors. Thus, the major effect of the electron-rich substituents at the meso-positions of the porphyrin ring is concluded to be the stabilization of the polar transition state rather than the destabilization of O–O bond by pushing electrons into the σ^* orbital of the peroxide. Acceleration of the homolysis of the O–O bond in **5** by depressing the polar transition state has been observed when a series of substituted perbenzoic acids were employed ($\rho = -0.4$).[11c]

In conclusion, it has been shown that the manners of push effect on homolysis and heterolysis are very different. A strong electron donor destabilizes the O–O bond (push effect) by pushing electrons into the antibonding orbitals of peroxide. At the same time, the push effect encourages the polar transition state. These effects obviously favor heterolysis of the O–O bond in **5**. On the other hand, the latter effect upsets homolysis. Thus, the appearance of the push effect on homolysis is not simple, i.e., the push effect by the sixth ligand is much less than the on heterolysis. More importantly, opposite effects on heterolysis and homolysis were observed upon changing substituents at the meso-positions or porphyrin ring. These observations are quite suggestive of biological utilization of strong electron-donor ligands in heme enzymes such as peroxidase, P-450, and catalase.